Available online at www.sciencedirect.com
SCIENCE DIRECT®
Journal of Geometry and Physics 56 (2006) 1875–1892
JOURNAL OF GEOMETRY AND PHYSICS
www.elsevier.com/locate/jgp

# Two-dimensional Lagrangian singularities and bifurcations of gradient lines II☆

G. Marelli

*Department of Mathematics, Kyoto University, Kitashirakawa, Sakyo-ku, Kyoto 606-8502, Japan*

Received 16 September 2005; accepted 19 October 2005
Available online 13 December 2005

**Abstract**

Motivated by mirror symmetry, we consider the Lagrangian fibration $\mathbb{R}^4 \to \mathbb{R}^2$ and Lagrangian maps $f : L \hookrightarrow \mathbb{R}^4 \to \mathbb{R}^2$, exhibiting an unstable singularity, and study how the bifurcation locus of gradient lines, the integral curves of $\nabla f_x$, for $x \in B$, where $f_x(y) = f(y) - x \cdot y$, changes when $f$ is slightly perturbed. We consider the cases when $f$ is the germ of a fold, of a cusp and, particularly, of an elliptic umbilic.


*MSC:* 37G25; 53D12; 70K60

*Keywords:* Lagrangian singularities; Bifurcation theory; Mirror symmetry

## 1. Introduction

This is the second of two papers motivated by the problem of quantum corrections in mirror symmetry. More precisely, in the first part [2], we considered the torus fibration $T^4 \to T^2$ and a Lagrangian map $f : L \hookrightarrow T^4 \to T^2$ exhibiting some unstable singularity, and studied how this singularity break when $L$ is slightly perturbed. We defined then the gradient lines of $f$ and examined some of their properties. Here instead we want to analyse, in a neighbourhood of the caustic of $f$, how the bifurcation locus of gradient lines changes when $L$ is perturbed. Since the problem is local, we can simply consider the Lagrangian fibration $\mathbb{R}^4 \to \mathbb{R}^2$. The study of the bifurcation locus of gradient lines for perturbations of $f$ is harder than the similar one, examined in [2], regarding the caustic: indeed, since the caustic is the set of critical values of $f$, the matter is, in a sense, local, while it is global when studying bifurcations of solutions of $\nabla f_x = 0$, since

☆ Supported by a JSPS postdoctoral fellowship.
*E-mail address:* marelli@kusm.kyoto-u.ac.jp.

0393-0440/$ – see front matter © 2005 Elsevier B.V. All rights reserved.
doi:10.1016/j.geomphys.2005.10.012

global aspects of the flow of a vector field are involved. The problem is relatively easy for the fold and the cusp, but it becomes much harder for perturbations of the elliptic umbilic, because, being its bifurcation locus non-empty, its complexity increases considerably when a small perturbation is added. The main result of this paper is Theorem 4.14, which is concerned with the bifurcation diagram of a small perturbation of the elliptic umbilic. The study of all these cases should help in drawing some ideas about the mutual positions of bifurcation lines and caustic.

## 2. The fold

The dynamical system (10) in [2], when $f$ is the generating function (2) in [2] of the fold in dimension 2, takes the form

$$\frac{\mathrm{d}y_1}{\mathrm{d}t} = y_1^2 - x_1, \qquad \frac{\mathrm{d}y_2}{\mathrm{d}t} = y_2 - x_2 \tag{1}$$

**Proposition 2.1.** $\mathcal{B} = \emptyset$.

**Proof.** The caustic has equation $x_1 = 0$. The vector fields (1) has respectively two, one or no critical points, depending on whether $x_1 > 0$, $x_1 = 0$ or $x_1 < 0$. If $x_1 > 0$ the critical points are $(\sqrt{x_1}, x_2)$ and $(-\sqrt{x_1}, x_2)$. Linearizing the vector field in a neighbourhood of these points, we find out that $(\sqrt{x_1}, x_2)$ has two positive eingenvalues, so it is an unstable node, while $(-\sqrt{x_1}, x_2)$ has a positive and a negative eigenvalue, so it is a saddle. Eq. (1) can be easily solved: there is a gradient line from the node to the saddle, which is generic and stable, and whose image is the segment with the node and the saddle as extremes. At $x_1 = 0$, on the caustic, the node and the saddle glue together in a saddle-node. □

## 3. The cusp

For the cusp

$$f(y_1, y_2) = \tfrac{1}{4}y_1^4 + y_1^2 y_2 + \tfrac{1}{2}y_2^2 \tag{2}$$

the dynamical system (10) in [2] has the form

$$\frac{\mathrm{d}y_1}{\mathrm{d}t} = y_1^3 + 2y_1 y_2 - x_1, \qquad \frac{\mathrm{d}y_2}{\mathrm{d}t} = y_1^2 + y_2 - x_2 \tag{3}$$

and the caustic is the semicubical parabola

$$|x_1| = \frac{4}{3}\sqrt{\frac{2}{3}}x_2^{3/2}$$

defined for $x_2 \geq 0$.

**Proposition 3.1.** *The bifurcation diagram of a small perturbation of the cusp, supported on a sufficiently small compact set $W$, has the following features, outlined in* Fig. 1:

1. *for* $|x_1| > \frac{4}{3}\sqrt{\frac{2}{3}}x_2^{3/2}$ (“*outside*” *the caustic*), $\nabla f_x$ *has only one critical point*: *a saddle*;
   *for* $|x_1| < \frac{4}{3}\sqrt{\frac{2}{3}}x_2^{3/2}$ (“*inside*” *the caustic*), $\nabla f_x$ *has three critical points*: *two saddles*, $s_1$ *and* $s_2$, *and a node* $n$;

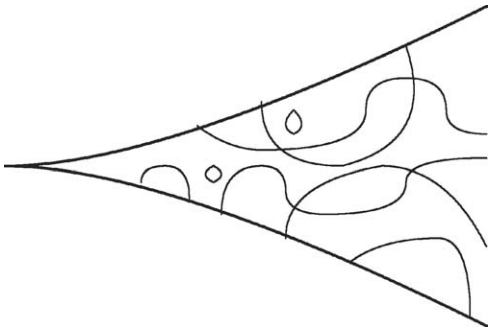

Fig. 1. The bifurcation diagram of a small perturbation of the cusp.

*for* $x_1 = \frac{4}{3}\sqrt{\frac{2}{3}}x_2^{3/2}$ (*the* $l_1$ *branch of the caustic*), $\nabla f_x$ *has two critical points*: *the saddle* $s_2$ *and the saddle-node* $ns_1$;

*for* $x_1 = -\frac{4}{3}\sqrt{\frac{2}{3}}x_2^{3/2}$ (*the* $l_2$ *branch of the caustic*), $\nabla f_x$ *has two critical points*: *the saddle* $s_1$ *and the saddle-node* $ns_2$;

*at* $(0, 0)$ (*the vertex of the cusp*), $\nabla f_x$ *has a degenerate* critical point $ns_1s_2$;

2. *if non-empty*, $\mathcal{B}$ *lies inside the caustic*; *moreover there exist a neighbourhood* $U$ *of the vertex of the cusp inside the caustic such that* $U \cap \mathcal{B} = \emptyset$; *in* $W$, $\mathcal{B}_{ij}$, *if non-empty*, *can contain lines*, *half-lines with origin at a point of* $l_i$, *segments with both the extremes on* $l_i$ *or immersed* $S^1$*'s*; $\mathcal{B}_{ij} \cap \mathcal{B}_{ji} = \emptyset$, *while two components* $\mathcal{B}^1_{ij}$ *and* $\mathcal{B}^2_{ij}$ *of* $\mathcal{B}_{ij}$ *can intersect provided the saddle-to-saddle separatrices* $\gamma_{s_is_j}$ *of the vector fields corresponding to points of* $\mathcal{B}^1_{ij}$ *and* $\mathcal{B}^2_{ij}$ *are obtained as intersection of the same pair of separatrices of* $s_1$ *and* $s_2$.

Note that, while Lagrangian equivalent maps have diffeomorphic caustics, their bifurcation loci in general are not diffeomorphic. Note also that no bifurcation line has the vertex of the cusp as limit point.

**Proof.**

1. All the statements follow from a direct computation of roots of $\nabla f_x$ and from the study of the sign of eigenvalues of the linearization of $\nabla f_x$ in a neighbourhood of its critical points.
2. Bifurcation points, if they exist, lie only inside the caustic, where at least two saddles exist. Since, if non-empty and far from the caustic, the components of $\mathcal{B}_{ij}$ are immersed submanifold of codimension 1, it follows that they can be either lines, half-lines with origin on the caustic, segments with extremes on the caustic, or immersed $S^1$'s.

Suppose $\bar{\mathcal{B}}_{ij} \cap l_j \neq \emptyset$ and take $p \in \bar{\mathcal{B}}_{ij} \cap l_j$, then, by Proposition (4.14) in [2], there exists an open subset $V$ such that $p \in \partial V$ and the phase portrait of $\nabla f_x$, for $x \in V$, does not exhibit the gradient line $\gamma_{ns_j}$; when $x$ moves along a path in $V$ ending at $p$, $n$ and $s_j$ glue together at $p$ forming the degenerate critical point $ns_j$, and so in the phase portrait of $\nabla f_p$ there would be two gradient lines with opposite directions joining $ns_j$ and $s_i$, which is not possible, as shown in the proof of Corollary (4.13) in [2].

Suppose the vertex $v$ of the cusp belongs to $\bar{\mathcal{B}}$, then moving along paths ending at $v$ contained into different connected components determined by $\mathcal{B}$, the phase portrait of $\nabla f_v$ would depend on these paths, giving a contradiction.

The statement about the intersection of components of $\mathcal{B}$ is a consequence of Corollary (4.18) in [2].

Finally, if $W$ is sufficiently small, Theorem (4.30) in [2] ensures in $W$ the existence of a generating function having a bifurcation diagram with such features. □

## 4. The elliptic umbilic

Consider the elliptic umbilic in dimension 2, whose generating function is

$$f(y_1, y_2) = y_1^3 - y_1 y_2^2 \tag{4}$$

The system (10) in [2] takes the form

$$\frac{\mathrm{d}y_1}{\mathrm{d}t} = y_1^2 - y_2^2 - x_1, \qquad \frac{\mathrm{d}y_2}{\mathrm{d}t} = -2y_1 y_2 - x_2 \tag{5}$$

**Proposition 4.1.** *The bifurcation locus $\mathcal{B}$ of (5) consists of three half-lines, with equations given by $t \to t\,\mathrm{e}^{i\alpha}$, for $\alpha = 0, 2\pi/3, 4\pi/3$, and $t > 0$, and is represented in* Fig. 2.

**Proof.** For $(x_1, x_2) \neq (0, 0)$, system (5) has two critical points: the saddles $s_1$ and $s_2$

$$s_1 = \left( \sqrt{\frac{\sqrt{x_1^2 + x_2^2}}{2} + x_1}, -sgn(x_2)\sqrt{\frac{\sqrt{x_1^2 + x_2^2}}{2} - x_1} \right),$$

$$s_2 = \left( -\sqrt{\frac{\sqrt{x_1^2 + x_2^2}}{2} + x_1}, sgn(x_2)\sqrt{\frac{\sqrt{x_1^2 + x_2^2}}{2} - x_1} \right)$$

(on the caustic $(x_1, x_2) = (0, 0)$, $s_1$ and $s_2$ glue together in a two-fold saddle, also called saddle of multiplicity 2). Note that $s_1$ and $s_2$ are symmetric with respect to the origin. Moreover, let $(\rho, \theta)$ and $(r, \alpha)$ be polar coordinates in the $(y_1, y_2)$-plane and $(x_1, x_2)$-plane respectively; suppose $x_2 > 0$ for simplicity, then the phase of the saddles depends on the phase of the parameter $(x_1, x_2)$ as

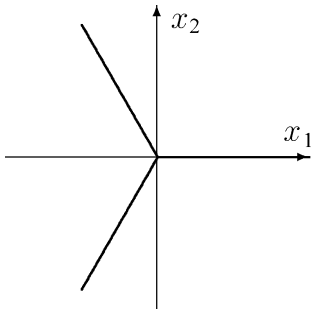


Fig. 2. The bifurcation diagram of the elliptic umbilic in dimension 2.

follows:

$$tg\,\theta = \frac{y_2}{y_1} = \frac{x_1}{x_2} - \sqrt{\left(\frac{x_1}{x_2}\right)^2 + 1} = \frac{\cos\alpha - 1}{\sin\alpha} = tg\left(-\frac{\alpha}{2}\right)$$

This means that rotating the point $(x_1, x_2)$ clockwise of an angle $\alpha$, the saddles rotate anti-clockwise of an angle $\alpha/2$. Observe also that system (5) can be scaled, in the sense that, if $y(t)$ is a solution of (5) corresponding to $x$, then $\tilde{y}(t) = \frac{1}{\lambda}y(\frac{t}{\lambda})$ is a solution of (5) corresponding to $x/\lambda^2$. So if a saddle-to-saddle separatrix exists for a given $x$, then it exists also for a positive multiple of $x$. This implies that the bifurcation locus is formed by rays with source in $(0, 0)$.

Note also that if $y(t)$ is a solution of (5) then $-y(t)$ is also a solution of (5). In particular, if a saddle-to-saddle separatrix exists, being the two saddles symmetric with respect to the origin, it implies that the saddle-to-saddle separatrix itself is symmetric with respect to the origin.

In polar coordinates, the generating function is written as

$$f(\rho, \theta) = \rho^3 \cos\theta\left(\tfrac{1}{3}\cos^2\theta - \sin^2\theta\right)$$

and (5) as

$$\frac{\mathrm{d}\rho}{\mathrm{d}t} = \rho^2\cos(3\theta) - r\,\cos(\theta - \alpha), \qquad \frac{\mathrm{d}\theta}{\mathrm{d}t} = \rho^2\sin(3\theta) + r\,\sin(\theta - \alpha) \tag{6}$$

We look for solutions through the origin whose image is a straight line, imposing the condition $\theta$ constant. In order to get a non-constant solution, the second equation of (6) implies that

$$\sin(3\theta) = 0, \qquad \sin(\theta - \alpha) = 0 \tag{7}$$

These equations are solved by $\theta = k\pi/3$, with $k \in \mathbb{Z}$, and $\alpha = \theta + h\pi$, with $h \in \mathbb{Z}$. Only for $k$ even we get a saddle-to-saddle separatrix. So $\mathcal{B}$ contains at least the half-lines with phase $0$, $2\pi/3$ and $4\pi/3$. Numerical evidences suggest that no other half-line from the origin belongs to $\mathcal{B}$. □

**Remark 4.2.** Fukaya in [1] proposed a conjecture according to which the bifurcation locus is isotopic to a set of certain integral curves of the gradient field of the multivalued function

$$x \mapsto \int_{D^2} u^*\omega$$

where $u$ is a pseudo-holomorphic disc bounded by the fibre over $x$ and by the given Lagrangian submanifold. In this particular case the conjecture is verified.

The next step is to determine the bifurcation diagram when a small perturbation is added. A first result is Lemma 4.3, which gives information about the structure of the bifurcation locus outside a disc containing the caustic.

**Lemma 4.3.** *The bifurcation locus $\mathcal{B}(\tilde{f})$ of a small perturbation $\tilde{f} = f + f'$ of $f$ is, outside a compact subset $D$ containing the support of $f'$, diffeomorphic to the bifurcation locus $\mathcal{B}(f)$ of $f$.*

**Proof.** We reason as in Proposition 4.10. We repeat here again the argument. Let $x_0 \in \mathcal{B}(f) \setminus D$, and call $\gamma$ the saddle-to-saddle separatrix between the saddles $s_1(x_0)$ and $s_2(x_0)$ of $\nabla f_{x_0}$. Consider a transversal $\gamma^\perp$ to $\gamma$, identify $\gamma^\perp$ with some interval $(a, b)$, and set, for every point $x$, $h(x) = W^u(s_1(x)) \cap \gamma^\perp$ and $k(x) = W^s(s_2(x)) \cap \gamma^\perp$ (note that, since $x \ni D$, $f'_x = 0$, thus $s_1(x)$ and $s_2(x)$ are also saddles of $\nabla\tilde{f}_x$). This defines a map $\psi_f : U(x_0) \to \mathbb{R}$, $\psi_f(x) = h(x) - k(x)$, where $U(x_0)$ is a suitably small disc around $x_0$. The bifurcation locus is the subset $\psi_f^{-1}(0)$. Note that, since

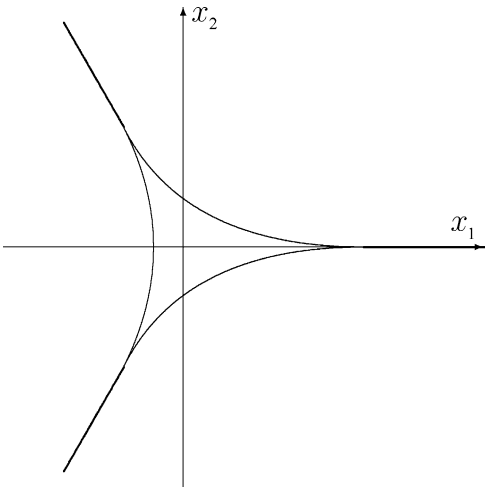


Fig. 3. The bifurcation diagram of a perturbation of the elliptic umbilic by a polynomial of degree 2.

$U(x_0) \setminus \psi_f^{-1}(0)$ has two connected component corresponding to different signs of $\psi_f$, the map $\psi_{\tilde{f}}$, defined for a small perturbation $\tilde{f}$ of $f$, still attain the value 0 at a certain point $\tilde{x}$. Moreover, since $\psi$ is a submersion at $x_0$, it is transversal to 0, and the point $\tilde{x}$ is unique. □

It remains to study the bifurcation diagram near the caustic. We proceed by first determining the allowed bifurcation diagrams, then Theorem (4.30) in [2] will ensure the existence of perturbations of $f$ exhibiting such diagrams. As a first step, consider a perturbation given by a polynomial of degree 2, for example $f'(y_1, y_2) = \frac{1}{2}(y_1^2 + y_2^2)$: the generating function is

$$\tilde{f}(y_1, y_2) = \tfrac{1}{3}y_1^3 - 2y_1y_2^2 + \tfrac{1}{2}(y_1^2 + y_2^2) \tag{8}$$

and (5) becomes

$$\frac{\mathrm{d}y_1}{\mathrm{d}t} = y_1^2 - y_2^2 + y_1 - x_1, \qquad \frac{\mathrm{d}y_2}{\mathrm{d}t} = -2y_1y_2 + y_2 - x_2 \tag{9}$$

This is the only case where some computation is still feasible.

**Proposition 4.4.** *The bifurcation locus of* (8) *contains at least three half-lines departing from each vertex of the caustic, given by* $t \to t\,\mathrm{e}^{i\alpha}$, *for* $\alpha = 0, 2\pi/3, 4\pi/3$, $t > 0$, *and represented in* Fig. 3.

**Proof.** If $x_2 = 0$ we find the following critical points: $s_1 = \left(\frac{1}{2}, \sqrt{\frac{3}{4} - x_1}\right)$ and $s_2 = \left(\frac{1}{2}, -\sqrt{\frac{3}{4} - x_1}\right)$, defined for $x_1 \le \frac{3}{4}$, and $s_3 = \left(\frac{-1-\sqrt{1+4x_1}}{2}, 0\right)$ and $n = \left(\frac{-1+\sqrt{1+4x_1}}{2}, 0\right)$, defined for $x_1 \ge -\frac{1}{4}$. Linearizing (9) at these points, we see that $s_1$, $s_2$ and $s_3$ are saddles, while $n$ is an unstable node for $-\frac{1}{4} \le x_1 < \frac{3}{4}$ and a saddle for $x_1 > \frac{3}{4}$. The points $s_1$, $s_2$ and $n$ at $x_1 = \frac{3}{4}$, a vertex of the tricuspoid, glue together into a degenerate critical point, which, for $x_1 > \frac{3}{4}$, turns into a simple (non-degenerate) saddle. Instead, at $x_1 = -\frac{1}{4}$, $s_3$ and $n$ glue together into a saddle-node, which disappears for $x_1 \ge -\frac{1}{4}$. This implies that, for $(x_1, x_2)$ inside the caustic, system (9) has four critical points, three saddles and an unstable node, while outside the caustic there are two

saddles. On each side of the caustic the node glues together with one of the three saddles, forming a degenerate critical point which disappears outside the caustic.

A gradient line $\gamma_{ns_3}$ from $n$ to $s_3$ can be explicitly computed, implying that the half-line $x_2 = 0$, $x_1 > \frac{3}{4}$, belongs to the bifurcation locus: setting $p = \frac{-1+\sqrt{1+4x_1}}{2}$ and $q = \frac{-1-\sqrt{1+4x_1}}{2}$, and choosing as initial condition a point on the $y_1$-axis between $p$ and $q$, for example 0, $\gamma_{ns_3}$ is given by

$$y_1(t) = pq\frac{1 - \mathrm{e}^{(p-q)t}}{q - p\,\mathrm{e}^{(p-q)t}}, \qquad y_2(t) = 0$$

The existence of the remaining bifurcation half-lines, having the other vertexes of the caustic as limit point, can be proved in a similar way. □

**Corollary 4.5.** *If $f'$ is a generic polynomial of degree 2, up to translations, the bifurcation diagram of $\tilde{f} = f + f'$ is represented in* Fig. 3.

**Proof.** As done in Subsection (3.1) of [2], we can reduce to the hypothesis of Proposition 4.4 as a consequence of a suitable translation. □

Before analysing a generic small perturbation of the elliptic umbilic (4), consider a generic small perturbations of (8).

**Proposition 4.6.** *The bifurcation locus of a small perturbation of* (8), *shown in* Fig. 4, *has the following features*:

1. *outside a compact subset containing the caustic $K$, there exist three bifurcation lines* (*as for the unperturbed elliptic umbilic*);
2. *generically, these half-lines intersect $K$ at a point of one of its sides near a vertex and have as extreme a fold point on the opposite side of $K$, near the same vertex*;
3. *as already described for the cusp in* Proposition 3.1, *inside $K$ also immersed $S^1$'s or segments, with extremes on the same side of $K$, may appear as components of the bifurcation locus*;

**Proof.** The structure of the bifurcation locus far from $K$, as described at point 1, is a direct consequence of Lemma 4.3. This, together with Proposition (4.10) in [2], implies that the bifurcation locus contains half-lines with extreme on the caustic. If $x$ is a cusp (a vertex) of $K$, then $\nabla\tilde{f}_x$ has a saddle $s_i$ and a degenerate critical point $ns_js_k$. Suppose a bifurcation line $\mathcal{B}$ has $x$ as limit point, then, for all $t \in \mathcal{B} \cap N$, where $N$ is a neighbourhood of the vertex $x$, the field $\nabla\tilde{f}_t$ exhibits a saddle-to-saddle separatrix $\gamma_t$, and, at the limit point $x$, a gradient line $\gamma_v$ exists between $s_i$ and $ns_js_k$. Since $\gamma_t$ is unstable, also $\gamma_v$ is unstable. Thus, generically, the limit point of a bifurcation line is a fold of $K$. That a bifurcation half-line $\mathcal{B}$ intersects $K$ on a side $l_i$ and has a limit point on one of the opposite sides $l_j$, is a consequence of the fact that the exceptional gradient line $\gamma_{s_js_k}$, exhibited by $\nabla\tilde{f}_x$ for $x \in \mathcal{B}$, breaks when one of the points $s_j$ or $s_k$ glues together with the node $n$ in a saddle-node, but this happens just when $x$ belongs to one of the opposite sides to $l_i$. The argument to prove point 3 is the same given for the cusp in Proposition 3.1. The proposition now follows from Theorem (4.30) in [2]. □

The final step is to determine the bifurcation locus of a generic perturbation of (4). The behaviour of the bifurcation locus outside the caustic is determined by Lemma 4.3. The idea to study how the bifurcation locus looks inside the caustic $K$ is as follows: we consider diagrams representing all the possible mutual positions of three bifurcation half-lines inside $K$, having an extreme

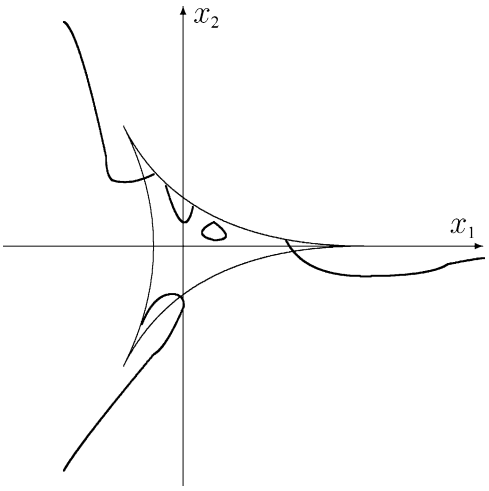


Fig. 4. The bifurcation diagram of a small perturbation of a perturbation by a polynomial of degree 2 of the elliptic umbilic.

on a certain side of $K$ and intersecting further $K$ at a point of the remaining sides, first assuming that such lines do not intersect, and we study which among such diagrams are allowed; then we do the same assuming bifurcation lines can intersect; finally, Theorem (4.30) in [2] ensures the existence of a function $\tilde{f}$ giving rise to such bifurcation diagrams.

As before we denote by $n$ and $s_i$, $i = 1, 2, 3$, the node and the saddles of $\nabla \tilde{f}_x$, for $x$ lying inside the caustic. Let $l_i$, for $i = 1, 2, 3$, be the side of the caustic where the saddle $s_i$ glues together with $n$. Observe that if a bifurcation half-line $\mathcal{B}$ intersects the side $l_i$ of the caustic and has its extreme on the opposite side $l_j$, it means that, for $x \in \mathcal{B}$, $\nabla \tilde{f}_x$ exhibits in its phase portrait the saddle-to-saddle separatrix $\gamma_{s_j s_k}$, from $s_j$ to $s_k$, with $k \in \{1, 2, 3\} \setminus \{i, j\}$: in other words, $\mathcal{B} \subset \mathcal{B}_{jk}$. Assume that bifurcation lines do not intersect. In this case, all the possible diagrams are drawn in Fig. 5.

**Lemma 4.7.** *Among diagrams in* Fig. 5, *only* (*A*), (*B*), (*C*), (*D*), (*G*), (*L*), (*M*), (*N*) *are allowed.*

**Proof.** In all diagrams, the subset $*$ is the one bounded by all the sides of the caustic. For every $x \in *$, the phase portrait of $\nabla \tilde{f}_x$ contains all the gradient lines $\gamma_{ns_i}$, $i = 1, 2, 3$: indeed, as already explained in the proof of Proposition 3.1, if $\gamma_{ns_i}$ were missing, then, for $x$ belonging to the side $l_i$ of the caustic bounding $*$, $\nabla \tilde{f}_x$ would exhibit two gradient lines between the $ns_i$ and one of the remaining saddles, implying a contradiction. The lemma follows now from Proposition (4.19) in [2] with considerations as those in Subsection (4.5) of [2]. □

We study now the possibility of intersection between bifurcation lines. The possible intersections, depending on the positions of bifurcation lines, are listed in Fig. 6.

In all these diagrams, the third bifurcation half-line, which is not shown, has a position such that the resulting bifurcation diagram is among those allowed by Lemma 4.7. In what follows, $l_1$ denotes the left side of the caustic, $l_2$ its upper side and $l_3$ its lower side.

Consider (a) (see Fig. 7).

**Proposition 4.8.** *The intersection of bifurcation lines of* (*a*) *gives an allowed bifurcation diagram provided* $\nabla \tilde{f}_x$ *exhibits, at points of both bifurcation lines, a saddle-to-saddle separatrix obtained by joining the same pair of separatrices.*

**Proof.** The result follows from Lemma (4.18) in [2]. At points of bifurcation lines the gradient line $\gamma_{s_2 s_1}$ appears in the phase portrait of $\nabla \tilde{f}_x$, however this can occur in three ways:

(1) the non-generic gradient line $\gamma_{s_2 s_1}$ in both bifurcations is obtained by joining the same pair of separatrices; the phase portrait of $\nabla \tilde{f}_x$ for $x \in \alpha$ is the same as the one for $x \in \gamma$ and it contains the gradient line $\gamma_{n s_1}$, which disappears for $x \in \beta$ (see Fig. 8);

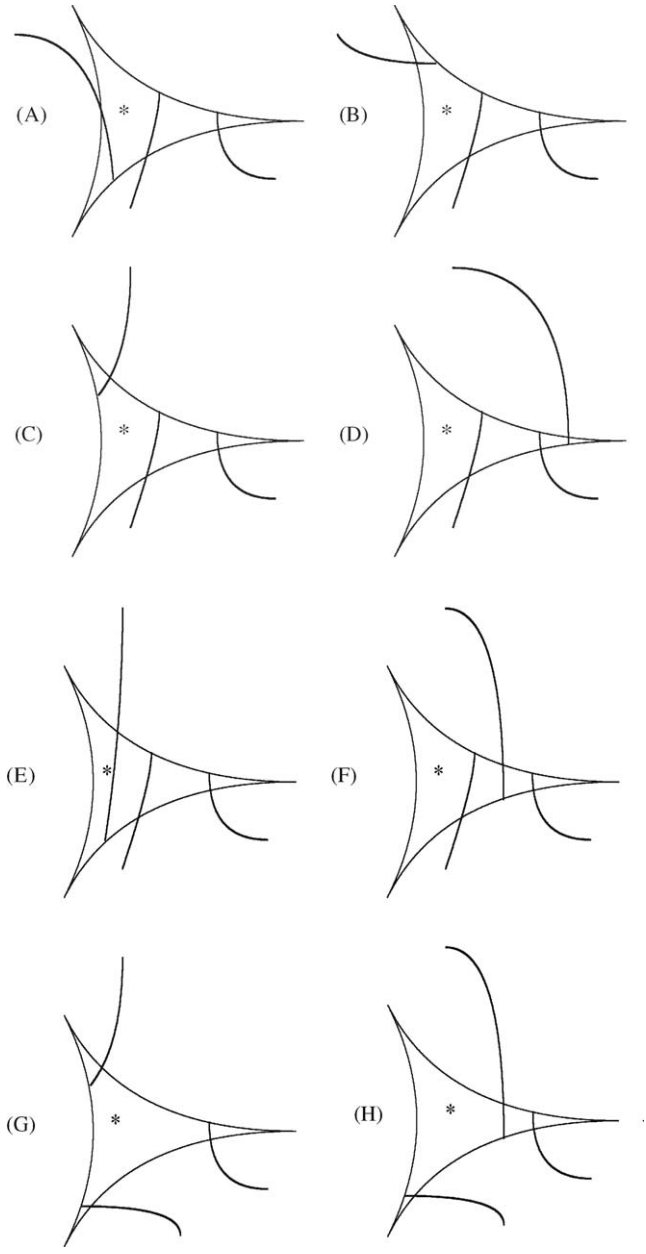


Fig. 5. Possible mutual positions of non-intersecting bifurcation lines inside the caustic.

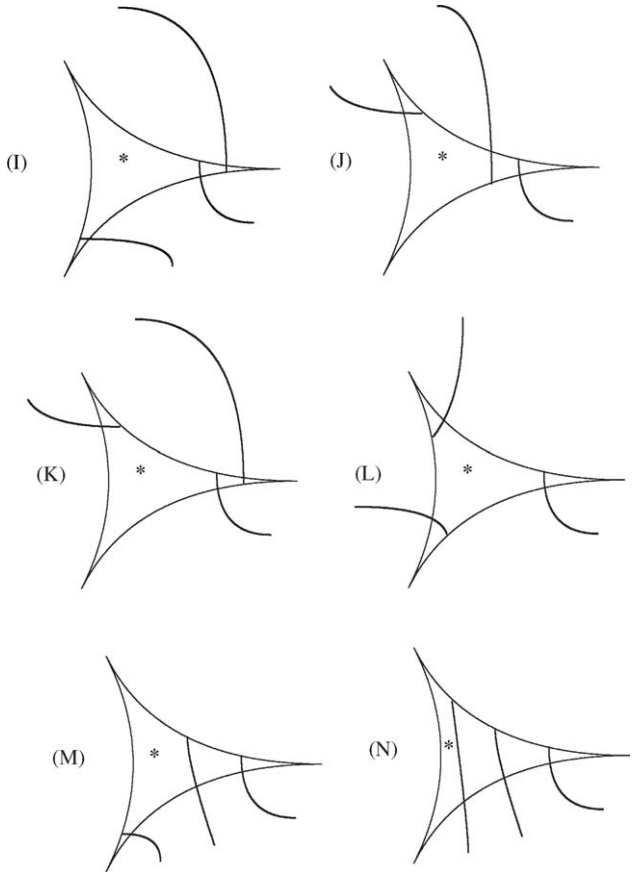


Fig. 5. (*Continued*).

(2) the non-generic gradient line $\gamma_{s_2 s_1}$ is obtained by joining different pairs of separatrices; the phase portrait of $\nabla \tilde{f}_x$ for $x \in \alpha$ differs from the one for $x \in \gamma$ (see Fig. 9);
(3) the non-generic gradient line $\gamma_{s_2 s_1}$ in both bifurcations is obtained by joining the same pair of separatrices; the phase portrait of $\nabla \tilde{f}_x$ for $x \in \alpha$ is the same as the one for $x \in \gamma$ and it never contains the gradient line $\gamma_{ns_1}$ (see Fig. 10).

The intersection is allowed only in cases (1) and (3). The phase portrait of $\nabla \tilde{f}_x$ for $x \in \delta$ is equivalent to the one of $\nabla \tilde{f}_x$ for $x \in \beta$. □

Consider (b) (see Fig. 11)

**Proposition 4.9.** *The intersection of bifurcation lines of* (*b*) *gives rise to an allowed bifurcation diagram.*

**Proof.** The phase portrait of $\nabla \tilde{f}_x$, for $x$ in $\alpha$, exhibits all the gradient lines $\gamma_{ns_i}$, for $i = 1, 2, 3$, because $\alpha$ is bounded by all the sides $l_i$ of the caustic (see Fig. 12).

The phase portrait of $\nabla \tilde{f}_x$, for $x$ in $\beta$ and for $x$ in $\gamma$, are represented in figure below: from $\alpha$ to $\beta$ the gradient line $\gamma_{s_2 s_1}$ appears and $\gamma_{ns_1}$ breaks; from $\alpha$ to $\gamma$ the gradient line $\gamma_{s_2 s_3}$ appears and $\gamma_{ns_3}$ breaks (see Fig. 13).

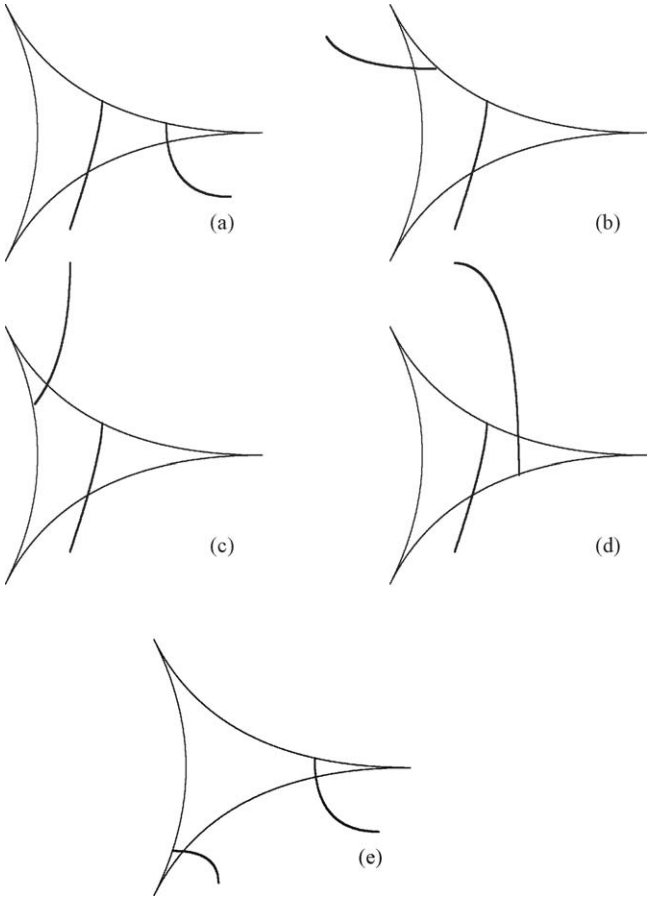


Fig. 6. Possible cases of intersection of bifurcation lines.

The bifurcations from $\beta$ to $\delta$ and from $\gamma$ to $\delta$, in principle, can occur into two different ways, as explained in Section (4.5) of [2]. However, the way gradient lines $\gamma_{ns_3}$ and $\gamma_{ns_1}$ wind around the node to provide the bifurcations is fixed by the phase portrait of $\nabla \tilde{f}_t$, where $t$ is the intersection point of the bifurcation lines. This is in turn determined by the bifurcations from $\alpha$ to $\beta$ and from $\alpha$ to $\gamma$, and showed in Fig. 14.

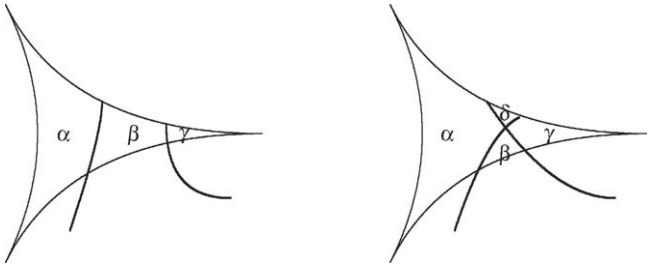


Fig. 7. Intersection of bifurcation lines: case (a).

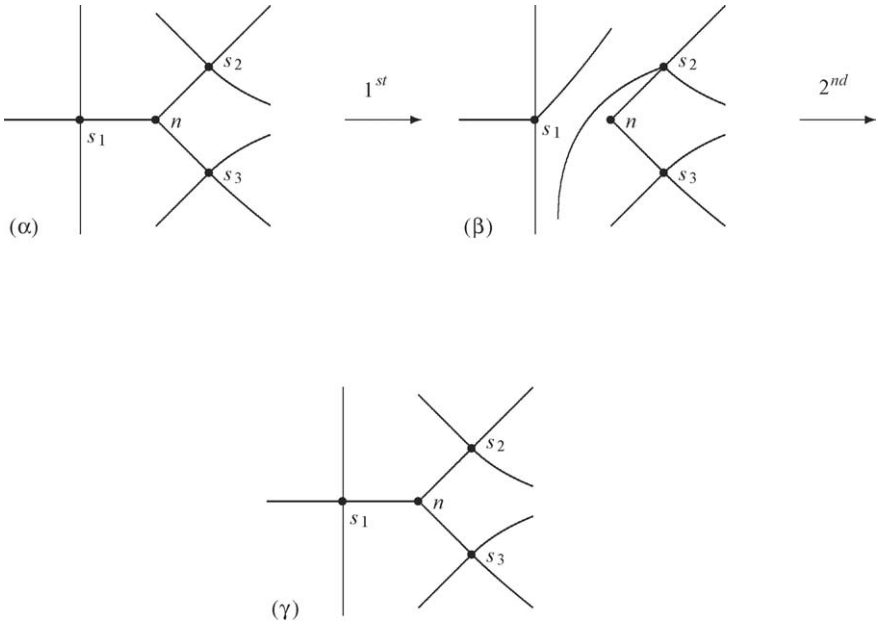


Fig. 8. The bifurcation from $\alpha$ to $\beta$ and from $\beta$ to $\gamma$, respectively: 1st possibility.

The phase portrait of $\nabla \tilde{f}_x$, for $x$ in $\delta$, is unambiguously determined (and shown in Fig. 15). The intersection is permitted.

Consider now (c) (see Fig. 16). □

**Proposition 4.10.** *Bifurcation lines of case* (*c*) *can intersect, however the new bifurcation diagram is allowed provided it also contains a new bifurcation line, from the intersection point to* $l_2$ *and*

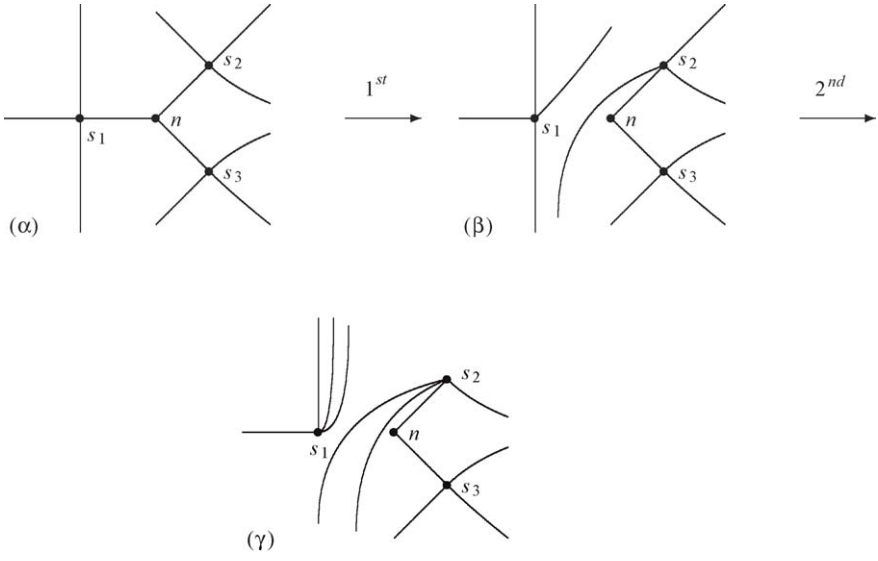


Fig. 9. The bifurcation from $\alpha$ to $\beta$ and from $\beta$ to $\gamma$, respectively: 2nd possibility.

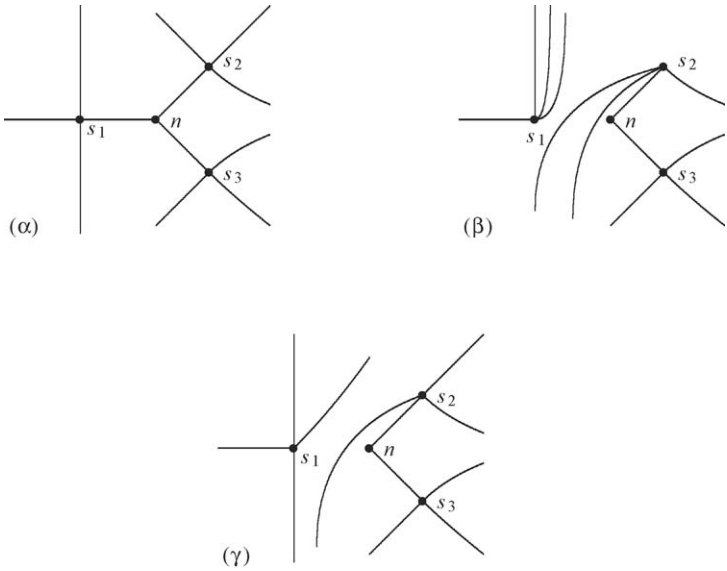


Fig. 10. The bifurcation from $\alpha$ to $\beta$ and from $\beta$ to $\gamma$, respectively: 3rd possibility.

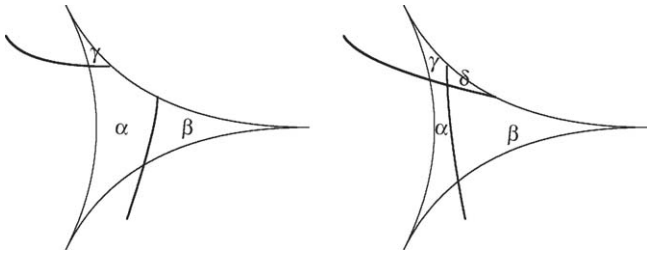


Fig. 11. Intersection of bifurcation lines: case (b).

*lying inside $\beta$, at whose points the phase portrait of $\nabla \tilde{f}_x$ exhibits a non-generic gradient line $\gamma_{s_1 s_3}$ from $s_1$* to *$s_3$. The bifurcation locus after the intersection is shown in* Fig. 17.

**Proof.** Whatever the position of the third bifurcation half-line is, the phase portrait of $\nabla \tilde{f}_x$, for $x$ in $\alpha$, exhibits all the gradient lines $\gamma_{ns_i}$, for $i = 1, 2, 3$ (see Fig. 18).

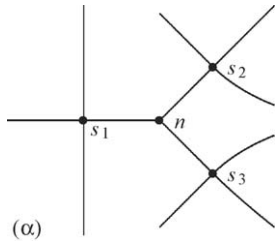


Fig. 12. The phase portrait of $\nabla \tilde{f}_x$ for $x \in \alpha$.

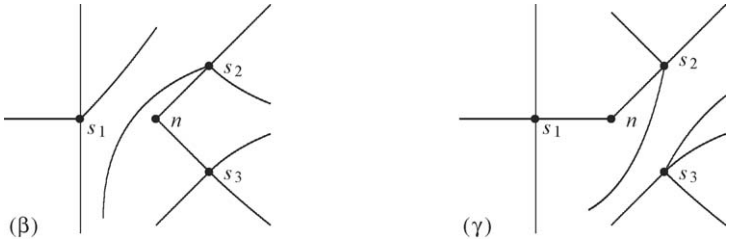


Fig. 13. The phase portrait of $\nabla \tilde{f}_x$ for $x \in \beta$ and $x \in \gamma$, respectively.

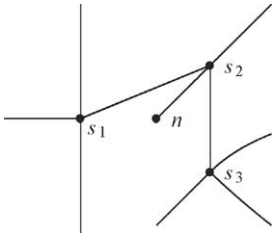


Fig. 14. The phase portrait of $\nabla \tilde{f}_t$ where $t$ is the intersection point of bifurcation lines.

There is only one way to perform the bifurcations from $\alpha$ to $\beta$ and from $\alpha$ to $\gamma$, obtaining the phase portrait showed in Fig. 19.

According to Proposition (4.19) in [2], in the phase portrait of $\nabla \tilde{f}_x$ for $x \in \beta$, shown in Fig. 19, a gradient line from $s_1$ to $s_3$ would provide a non-allowed diagram, so $\beta$ cannot be bounded by the bifurcation line, shown in Fig. 16, separating $\beta$ from $\delta$. In $\gamma$, instead, the gradient line $\gamma_{s_2 s_1}$ gives an allowed bifurcation diagram, so the bifurcation line separating $\gamma$ from $\delta$ is allowed. The bifurcation line separating $\delta$ from $\beta$ produces an allowed bifurcation diagram, because the gradient line $\gamma_{s_1 s_3}$ can appear in phase portrait $\delta$, though this implies for $x \in \beta$ a phase diagram of $\nabla \tilde{f}_x$ different from that shown in Fig. 19. However, as already explained in Subsection (4.6) of [2], we can suppose that the intersection point $t \in \mathcal{B}_{(2,1),(1,3)}$ belongs also to $\mathcal{B}_{2,3}$, so a new bifurcation line $\mathcal{B}'$ arises: $\mathcal{B}'$ is actually a segment with an extreme at the intersection point $t$ and the other extreme on $l_2$, where the saddle $s_2$ glues together with the node. At a point $x \in \mathcal{B}'$, a saddle-to-saddle separatrix $\gamma_{s_2 s_3}$ appears in the phase portrait of $\nabla \tilde{f}_x$. Since the problem is crossing the bifurcartion line from $\beta$ to $\delta$, we suppose that $\mathcal{B}'$ lies inside $\beta$. Call $\epsilon$ the new subset determined in the bifurcation diagram by $\mathcal{B}'$, lying between $\beta$ and $\delta$. At points of $\mathcal{B}'$, from $\beta$ to $\epsilon$, in principle there are two ways to perform the bifurcation, that is, $\gamma_{s_2 s_3}$ can be obtained by joining

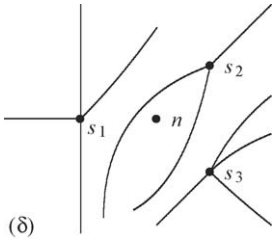


Fig. 15. The phase portrait of $\nabla \tilde{f}_x$ for $x \in \delta$.

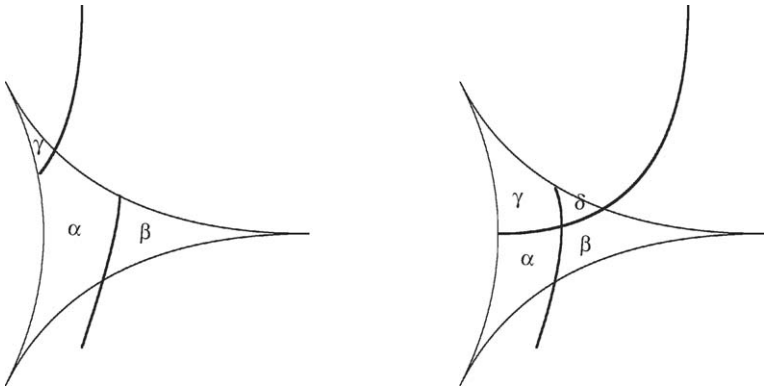


Fig. 16. Intersection of bifurcation lines: case (c).

two different pairs of separatrices, however the choice is fixed, and shown in Fig. 20, by the phase portrait of $\nabla \tilde{f}_t$, where $t$ is the intersection point of bifurcation lines (see Fig. 23).

The bifurcation from $\epsilon$ to $\delta$, being characterized by a non-generic gradient line $\gamma_{s_1 s_3}$ in the phase portrait of $\nabla \tilde{f}_x$, is allowed. Since such line appears in the phase portrait of $\nabla \tilde{f}_t$, where $t$ is the intersection point of bifurcation lines, the choice of the pair of separatices to be joined in $\gamma_{s_1 s_3}$ is thus determined (see Fig. 21).

For $x$ belonging to the bifurcation line separating $\delta$ from $\gamma$, a non-generic gradient line $\gamma_{s_2 s_1}$ must appear in the phase portrait of $\nabla \tilde{f}_x$: again, since such a line appears in the phase portrait of $\nabla \tilde{f}_t$, the choice of the pair of separatrices intersecting in $\gamma_{s_2 s_1}$ is fixed (see Fig. 22).

The phase portrait of $\nabla \tilde{f}_t$, where $t$ is the intersection point, is shown in Fig. 23. □

**Remark 4.11.** Observe that there are five ways to break the exceptional gradient lines appearing in the phase portrait of $\nabla \tilde{f}_t$, shown in Fig. 23, as five are the bifurcation lines arising from the intersection point in the bifurcation diagram in Fig. 16. Note that $\gamma_{s_2 s_1}$ and $\gamma_{s_1 s_3}$, as already explained in Subsection (4.6) of [2], can break in such a way to give rise to the exceptional gradient line $\gamma_{s_2 s_3}$, which is not exhibited by any of phase portraits of $\nabla \tilde{f}_x$, for $x$ belonging to the bifurcation lines, when these do not intersect.

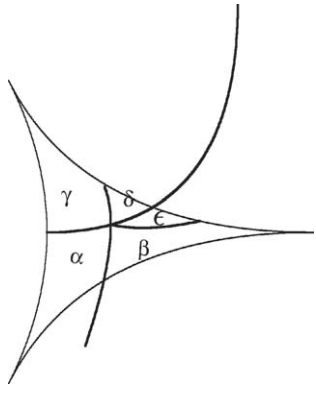


Fig. 17. The resulting bifurcation diagram after the intersection of bifurcation lines in case (c).

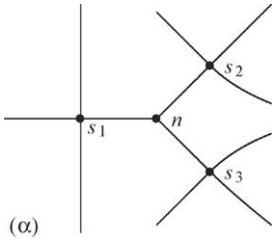


Fig. 18. The phase portrait of $\nabla \tilde{f}_x$ for $x \in \alpha$.

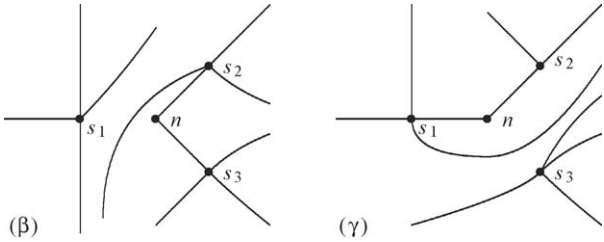


Fig. 19. The phase portrait of $\nabla \tilde{f}_x$ for $x \in \beta$ and $x \in \gamma$, respectively.

Consider now (d) (see Fig. 24). Among those in Fig. 5, the only allowed diagram exhibiting this configuration is (D).

**Proposition 4.12.** *The bifurcation diagram resulting from the intersection of bifurcation lines of* (*d*) *is not allowed.*

**Proof.** If the intersection were allowed, then the phase portrait of $\nabla \tilde{f}_t$, where $t$ is the intersection point, would exhibit the gradient lines $\gamma_{ns_2}$, $\gamma_{ns_3}$ and the non-generic gradient lines $\gamma_{s_2s_1}$ and $\gamma_{s_3s_1}$, but such a vector field does not exist. □

Consider (e) (see Fig. 25).

**Proposition 4.13.** *The bifurcation diagram resulting from the intersection of the bifurcation lines of* (*e*) *is not allowed.*

**Proof.** If the intersection were allowed, the phase portrait of $\nabla \tilde{f}_t$, when $t$ is the intersection point, would exhibit two non-generic gradient lines $\gamma_{s_1s_2}$ and $\gamma_{s_2s_1}$, giving a contradiction. □

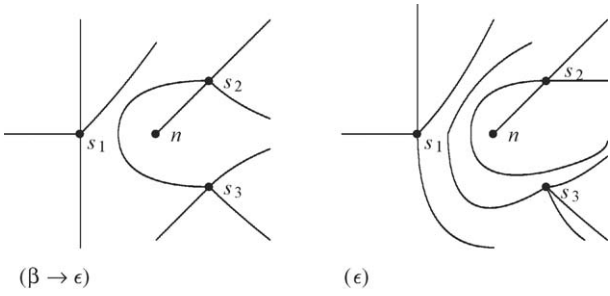


Fig. 20. The bifurcation from $\beta$ to $\epsilon$ and the phase portrait of $\nabla \tilde{f}_x$ for $x \in \epsilon$.

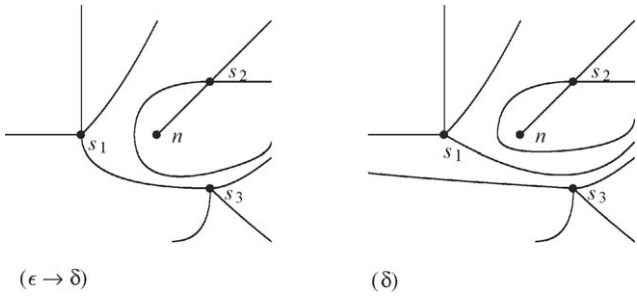


Fig. 21. The bifurcation from $\epsilon$ to $\delta$ and the phase portrait of $\nabla \tilde{f}_x$ for $x \in \delta$.

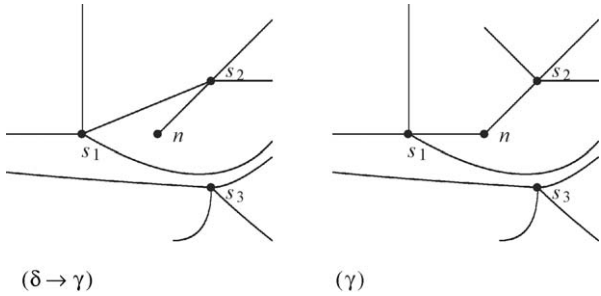


Fig. 22. The bifurcation from $\delta$ to $\gamma$ and the phase portrait of $\nabla \tilde{f}_x$ for $x \in \gamma$.

We realize that, inside the caustic, the bifurcation locus of a perturbation of the elliptic umbilic can be rather complex. We can resume all the results in the following theorem:

**Theorem 4.14.** *The bifurcation locus $\mathcal{B}$ of a small perturbation of the generating function (4) of the elliptic umbilic in dimension 2 has the following features*:

- *outside a compact subset containing the caustic K, $\mathcal{B}$ exhibits three bifurcation half-lines*;
- *generically, these half-lines intersect K along one of its sides and have their extreme at a fold point of one of the opposite sides*;
- *the allowed mutual positions of bifurcation lines and their possible intersections are described by Lemma 4.7 and by Propositions 4.8–4.13*;
- *inside K, $\mathcal{B}$ can also contain immersed $S^1$'s or segments, with extremes on the same side of K.*

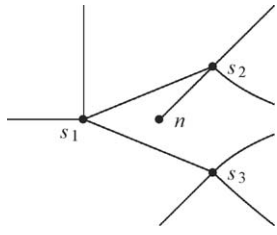


Fig. 23. The phase portrait of $\nabla \tilde{f}_t$ where $t$ is the intersection point of bifurcation lines.

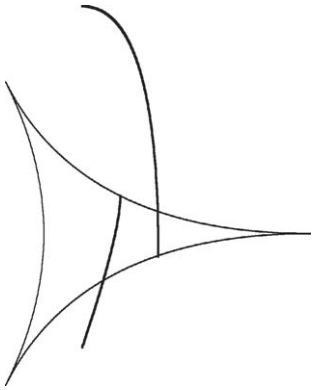

Fig. 24. Intersection of bifurcation lines: case (d).

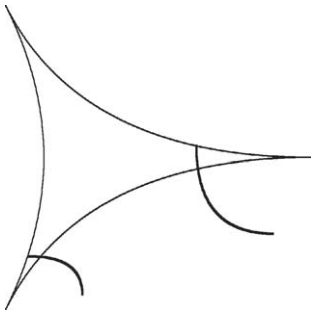

Fig. 25. Intersection of bifurcation lines: case (e).

## Acknowledgements

I wish to thank K. Fukaya, whose suggestions and help were decisive for the achievement of all the results here expounded. I am thankful to JSPS (Japan Society for the Promotion of Science) which awarded me with a JSPS postdoctoral fellowship at Kyoto University, where this paper was written.

## References

[1] K. Fukaya, Multivalued Morse theory, asymptotics analysis and mirror symmetry, 2002. Available from the web page http://www.math.kyoto-u.ac.jp/∼fukaya/fukayagrapat.dvi.
[2] G. Marelli, Two-dimensional Lagrangian singularities and bifurcations of gradient lines I, pre-print.